DEVELOPMENT OF A DRIVING ELECTRIC DYNAMOMETER ROTOR EMULATOR FOR MHK IN-STREAM TURBINES

William E. Laing, Jr.[a,b] James H. VanZwieten[b]

[a]Corresponding author: wlaing@fau.edu
[b]Southeast National Marine Renewable Energy Center, Florida Atlantic University, Boca Raton, FL, USA

ABSTRACT

As marine and hydrokinetic (MHK) technologies which convert the flow of fluid into useful electrical power are developed, it is desirable to simulate drivetrain performance and refine control strategies in a laboratory prior to field installation. This paper presents and evaluates a technique developed to operate the prime mover of a dynamometer so that it drives a machine under test like an MHK turbine's rotor. The approach utilizes environmental and rotor numerical models to calculate hydrodynamic torque. Relationships between shaft torque, shaft speed, and variable frequency drive native torque reference were used to modify torque reference settings to achieve actual emulated torque values. The accuracy at which physical shaft torque matches theoretical hydrodynamic torque was then evaluated for three basic operating states: locked rotor, spin up/down, and variable flow operation. Percent-error of averaged measured and theoretical shaft torque during simulation of these states was 9.7%, 5.5%, and 5.2%, respectively, demonstrating the success of applying the proposed technique.

I - INTRODUCTION

Two major projects to support the development of a commercial ocean current energy industry at the Southeast National Marine Renewable Center (SNMREC) include preparing a small scale ocean current research turbine (OCT) (Figure 1) and an associated 20-kW ocean current power generation simulator (OCPGS, Figure 2).

The OCT allows turbine component manufacturers to evaluate product performance using an open source, documented, and characterized platform. In addition, various research applications (e.g., prognostics and machine monitoring, corrosion and bio-fouling, rotor performance tools, etc.) are intended for the utility of the OCT.

Figure 1 – SNMREC's research OCT after preliminary sea trials during December 2013.

The OCPGS provides a laboratory-based controlled environment tool to evaluate and tune drivetrains for ocean current turbines. Specific applications include: developing and evaluating power takeoff control algorithms, quantifying generator performance [1], evaluating machine condition monitoring systems [2][3][4], and testing drivetrain hardware components prior to wet testing of OCTs.

Figure 2 - Photograph of SNMREC 20-kW dynamometer

Although dynamometer laboratory testing is commonplace, the key to applying this approach to MHK drivetrain optimization and testing is the development of a flexible and effective rotor emulation scheme. Rotor emulators have been utilized for wind turbine and MHK applications in the past, but involve customized hardware approaches to implement [5][6][7]. In addition, no emulators are available with configurations specific to ocean current environmental conditions.

Rotor and turbine emulators often use custom hardware in conjunction with transformations of governing electrical equations for direct electrical control of a driving motor. However, our approach assumes commercially available off-the-shelf VFDs are used for motor control. In order to achieve the same functionality as customized solutions, this project views the VFD and motor as a "black box" with torque reference as input and actual physical shaft torque as the output (Figure 3).

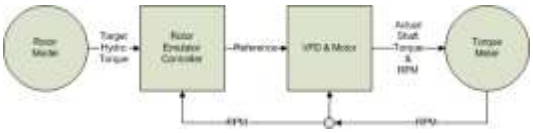

Figure 3 - Block Diagram for Rotor Emulator Controller

Section II describes the OCPGS platform in detail. Section III presents the approach developed to operate the prime mover of this dynamometer as a rotor emulator. In Section IV, evaluation of the rotor emulator is presented. Finally, conclusions are presented and suggestions are made for future work in Section V.

II - THE SNMREC DYNAMOMETER

The SNMREC has designed, installed, and is operating a variable-speed, variable-torque dynamometer (also referred to as a "dyno"), the Ocean Current Power Generation Simulator, or OCPGS (Figure 2). The prime mover, or driving side of the dyno, consists of a 20-kW Leeson alternating current (ac) squirrel-cage induction motor, a 26-kNm Bonfiglioli planetary gear with a 21.8:1 speed reduction, and controlled by a 30-hp US Drives variable frequency drive (VFD). At rated speed, the prime mover motor rotates at 1606 RPM, which is equivalent to a rotor shaft rotational speed of 73 RPM (after planetary gear reduction). An optical 1024 pulse-per-revolution GES encoder is installed on the high speed motor shaft and provides shaft rotation speed feedback to the VFD. The driving side of the dyno is used to emulate a rotor operating in a hydrodynamic flow (shaded area on the left in Figure 4). The prime mover was selected to deliver a range of hydrodynamic shaft torque that would be expected from the 3-meter diameter rotor of SNMREC's research OCT operating in the Florida Current.

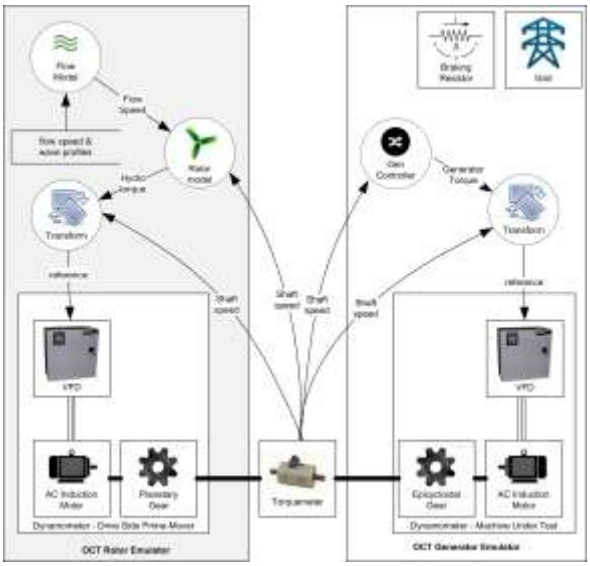

Figure 4 - Dynamometer block diagram

The driven end of a dynamometer is commonly referred to as the machine-under-test (MUT). In this study, the generator of the SNMREC experimental OCT (Figure 1) is installed as the MUT. This particular MUT is a 20-kW Sumitomo ac squirrel-cage induction motor and a 30-hp US Drives VFD. The designed rotational speeds of the rotor shaft are too slow for the ac induction motor to produce usable electric power, so a 1:25 ratio Sumitomo epicycloidal gear is coupled to the motor to increase rotational speed to match motor requirements. For example, in this configuration, at a rotor design speed of 50 RPM, the motor rotates at 1250 RPM.

Connecting the shafts of the prime mover and the MUT is a Himmelstein digital torquemeter used for the acquisition of rotor shaft speed, rotor shaft torque, and rotor shaft power. Dynamometer components are tested, monitored and controlled by software developed at the SNMREC. Rotor emulator control software communicates with the VFDs using Modbus protocol over TCP/IP, and a proprietary command-line interface over RS232 is used to communicate with the torquemeter.

III - ROTOR EMULATOR ARCHITECTURE

The hardware described in the previous section provides considerable flexibility in terms of how it can be configured. How the prime mover of the OCPGS is controlled influences how it can behave as an MHK rotor. Since the MUT in the study is intended to be installed in the SNRMEC's

OCT, the emulator scheme selected is the predicted operational behavior of its rotor (described in [8]). The rotor emulator's architecture (Figure 5) consists of both hardware components (rectangular shapes) and software components (circular shapes).

The software approach includes three major components: a flow model, a rotor model, and torque reference management. Software components are written in the LabVIEW® programming language [9] with some supporting functions developed with Matlab® [10]. The rotor emulator utilizes a timed-loop structure as its highest-level architectural component. For the present work, the main program executes one cycle each 150-millisecond time-step.

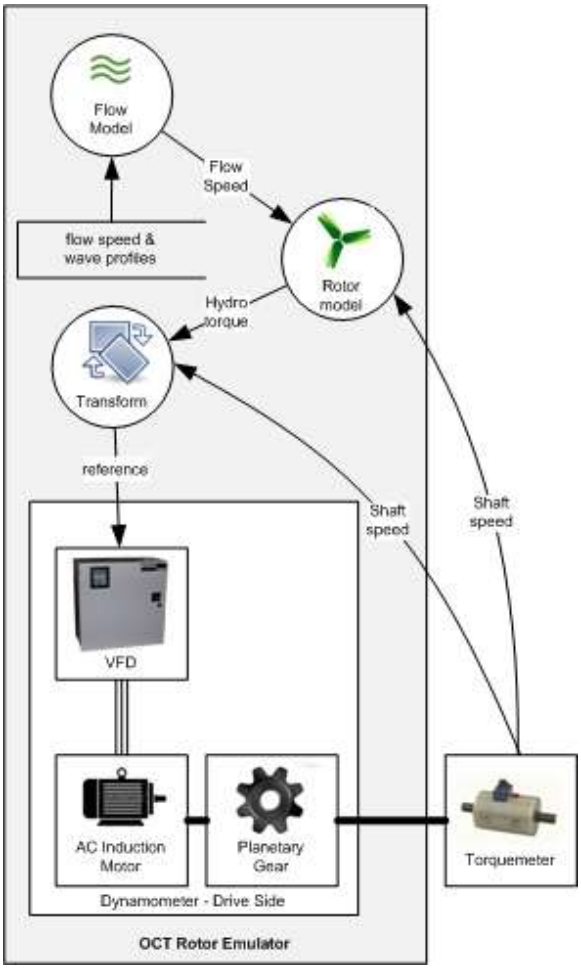

Figure 5 - Rotor emulator architecture

The Flow Model

The objective of the Flow Model (Figure 6) is to calculate a combined flow velocity value (for each execution cycle) for use by the rotor model. The flow model includes a base flow component (flow not caused by waves) that can either be set to a constant or imported as a time history. This base flow is then summed with wave perturbations which can be included in any of three methods: the horizontal component of wave orbital velocities calculated using a JONSWAP wave spectrum [11], a simple sinusoid, or a previously defined wave time history. If a JONSWAP wave spectrum is selected, user-specified significant wave height and turbine operating depths are utilized for defining the wave induced water velocity. The wave orbital velocity time history is calculated by summing individual wave components from the spectrum, assuming that they decay with depth according to linear wave theory [12]:

$$\sum_{i=1}^{N} \frac{H_i g k_i}{2\omega_i} \frac{\cosh(k_i(h-Z))}{\cosh(k_i h)} \cos(-\omega_i t + \phi_i), \qquad (1)$$

where H_i is the wave component amplitude, ω_i is the wave component frequency, k_i is the wave component number, ϕ_i is the random phase angle which is uniformly distributed from 0 to 2π and constant with time, h is the water depth, and t is time in seconds. This approach allows the calculated sea surface spectrum to determine appropriate perturbations at OCT hub heights.

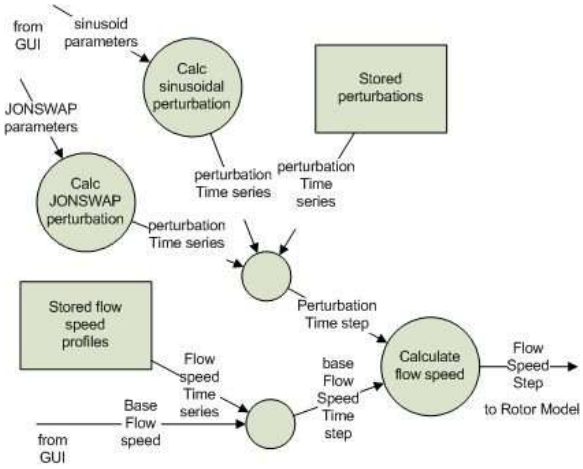

Figure 6 - Flow model structure

If a previously defined wave time history is used, a horizontal orbital water velocity for each time step at an OCT's hub height is required. Similarly, a simple sinusoidal orbital water velocity can be configured at an OCT hub height.

The Rotor Model

The rotor model calculates hydrodynamic torque based on the hydrodynamic characteristics of an MHK design (in this case, the SNMREC experimental OCT), using both axial flow and quasi-static approximations. The quasi-static inflow assumption, which assumes that the reduced flow upstream from the rotor has converged to the equilibrium value corresponding to the calculated rotor forces each time step,

dampens effects that abrupt changes in either rotor speed or free-stream velocity impart on torque. However, this approach does not affect steady-state torques and is therefore a reasonable first approach selected to achieve computational efficiency.

Hydrodynamic shaft torque is calculated as a function of both RPM and flow velocity. For this study, the SNMREC OCT rotor design, as presented in [5], is applied. This rotor model is based on quasi-steady hydrodynamic performance estimates calculated using the National Renewable Energy Laboratory's (NREL) WT_Perf open source public rotor code [13], which assumes the flow is axial. The rotor's airfoil family is the FX-77W airfoil [14] and the final foil shapes were optimized using NREL's HARPOpt [15] for a fixed rotational speed of 50 RPM. This particular design is predicted to have a mean shaft power of 7.405 kW, when operating in the Gulf Stream at a fixed speed of 50 RPM [8].

Predicted quasi-steady torque coefficients are found using the results from WT_Perf [13]. This coefficient is used to calculate the theoretical shaft torque, τ, according to:

$$\tau = C_\tau 0.5 \rho A V_o^2 R, \quad (2)$$

where ρ is the density of sea water, A is the swept area of the rotor, R is the radius of the rotor, and V_o is the free stream velocity. The resulting maximum torque coefficient is 0.121, which occurs at a tip speed ratio (TSR) of 3.45.

To calculate instantaneous hydrodynamic rotor torque for dynamometer use, free stream water velocity calculated by the flow model is used, and the RPM of the shaft is measured. Using these, the TSR is calculated from:

$$TSR = \frac{2\pi RPM\, R}{60 V_o}. \quad (3)$$

To avoid using a lookup table to determine a real-time shaft torque coefficient, polynomials were fit to this curve (Figure 7). Coefficients of torque were calculated at TSR increments of 0.1 using WT_Perf and the following 3rd-order polynomial was fit to these data, over the approximate region where the airfoils are stalled, from a TSR of 0 up to the TSR where the maximum C_τ occurs (TSR = 3.45):

$$C_\tau^{R1} = 0.00974 + 0.00958 \cdot TSR + 0.01403 \cdot TSR^2 - 0.00216 \cdot TSR^3. \quad (4)$$

For the range of TSR from 3.61 to 14.14, a second 3rd-order polynomial is fit to these data, and the resulting polynomial is:

$$C_\tau^{R2} = 0.21562 - 0.03370 \cdot \mathrm{TSR} + 0.00218 \cdot \mathrm{TSR}^2 - 0.00007 \cdot TSR^3. \quad (5)$$

To avoid discontinuities in the relationship between TSR and the estimated C_τ, linear interpolation is used for TSRs between 3.45 and 3.61. The relationship between TSR and C_τ is applied to dynamometer settings using the following logic statements:

$$\begin{cases} if\ TSR \le 3.45 & C_\tau^e = C_\tau^{R1}(\mathrm{TSR}) \\ if\ TSR \ge 3.61 & C_\tau^e = C_\tau^{R2}(\mathrm{TSR}) \\ else & C_\tau^e = \left(C_\tau^{R2}(3.61) - C_\tau^{R1}(3.45)\right)\frac{(TSR-3.45)}{0.16} \end{cases}. \quad (6)$$

The resulting C_τ^e is presented with C_τ in Figure 7. Hydrodynamic shaft torque is then calculated from C_τ^e by:

$$\tau_H = \left(0.5 \rho A {V_0}^2 R\right) \cdot C_\tau^e. \quad (7)$$

In this calculation, the density of sea water is assumed to be a constant 1025 kg/m^3.

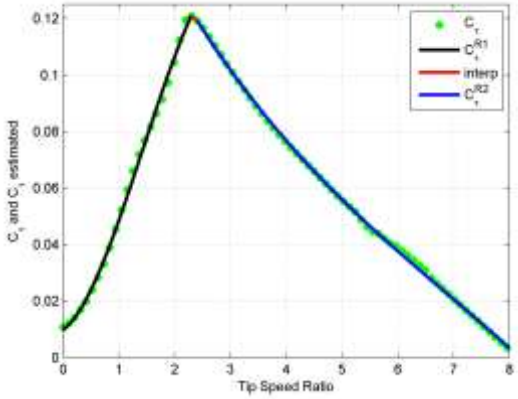

Figure 7 – Predicted hydrodynamic shaft torque coefficient presented as a function of TSR. The utilized discrete WT_Perf calculated torque coefficients, C_τ, are presented as well as the continuous estimated torque coefficient functions, C_τ^e.

Torque and VFD Torque Reference

Custom software was designed to control shaft torque by setting torque reference values for the prime mover's VFD (Figure 8).

Figure 8 – Prime mover variable frequency drive

In general, VFDs are controlled with speed or torque references. In torque control mode, a VFD uses motor shaft speed feedback from an encoder to achieve a commanded level of torque reference. For a magnetic field to be induced in the rotor of an ac induction motor, the rotor's speed must be different from the speed of the stator's magnetic field. Thus, ac induction motors are said to be asynchronous. The difference between stator speed, n_s, and rotor speed, n_r, is called slip, s, and is calculated as

$$s = \frac{n_s - n_r}{n_s}. \quad (8)$$

The motor develops maximum torque when slip is at its rated value. For the driving motor used in this project, rated speed at full load torque is 1775 RPM, while synchronous speed is 1800 RPM. So, the rated slip is

$$\frac{n_s - n_r}{n_s} = \frac{1800-1775}{1800} = 1.4\%. \quad (9)$$

In torque control mode, a VFD adjusts synchronous speed based on rotor speed, as reported by an encoder to achieve a target slip. In our study case, the VFD will attempt to achieve a rated slip of 1.4% when it is commanded a torque reference value of 100%. Greater torque reference values equate to greater pulling torque during motoring or greater resisting torque during regeneration.

The relationships between shaft torque and shaft rotational velocity are experimentally quantified over a range of ten evenly-spaced VFD torque references, from 10% to 100%. To enable the selection of appropriate torque reference values that are a function of both measured shaft RPM and desired shaft torque, 6th-order polynomials are used. Measured shaft speed is used by these polynomials to calculate shaft torque values for each of the 10 torque reference values. Spline interpolation with linear extrapolation is then used find the torque reference value that corresponds to the desired shaft torque value.

For each experimental run, to generate these data, the prime mover motor is commanded to a constant torque reference value. The generator-motor is then commanded through its range of shaft speed (from 0-60 RPM) using a slow angular acceleration rate of 0.01 rev./s^2, (at the slow speed shaft), so that nearly steady-state values are obtained. Example shaft torque data are presented in Figure 9 as a function of shaft RPM. After 6th-order polynomials are fit to each data set (Figure 9), the resulting R-squared values range between 0.855 and 0.967. At RPM values greater than 50 and at low shaft torque values (less than 1000 Nm), dynamometer torsional resonance effects are present. However, this range is not expected to be encountered in OCT operation, and was therefore only included for reference.

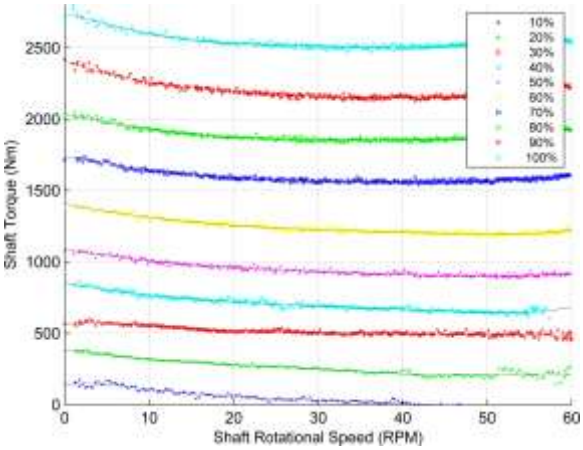

Figure 9 – Shaft torque presented as function of shaft speed for ten torque references.

To demonstrate the relationship between torque reference and shaft torque, the 10 data points that correspond to each of the shaft rotational velocities of 0, 20, 40, and 60 RPM are presented in Figure 10. This figure also demonstrates the corresponding interpolated values that would be chosen for these rotational velocities.

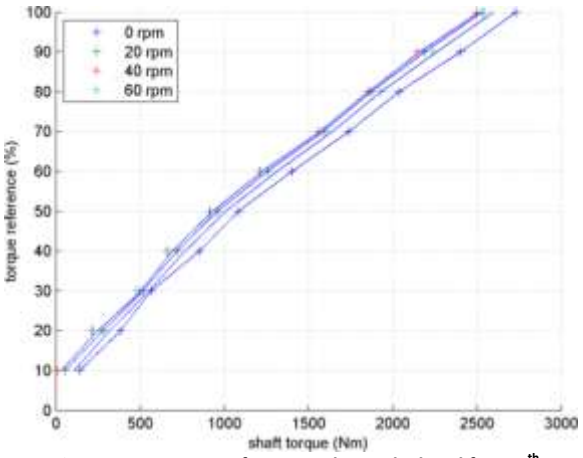

Figure 10 – Torque reference values calculated from 6th-order polynomials for RPMs of 0, 20, 40 and 60. The interpolated/extrapolated relationship between torque reference and shaft torque for these RPMs is also included.

The ability of this combined polynomial/interpolation mapping technique to represent the measured relationship between torque and torque reference was evaluated for RPMs of 0, 25, and 50. Figure 11 presents the full range of torque references (0%-100%) commanded to the VFD, associated measured torque imparted to the dynamometer's shaft by the rotor emulator motor, and the relationship predicted by the developed model. As can be

observed, the utilized mapping technique closely matches these recorded data over the entire range of VFD reference torques at three evaluated shaft speeds.

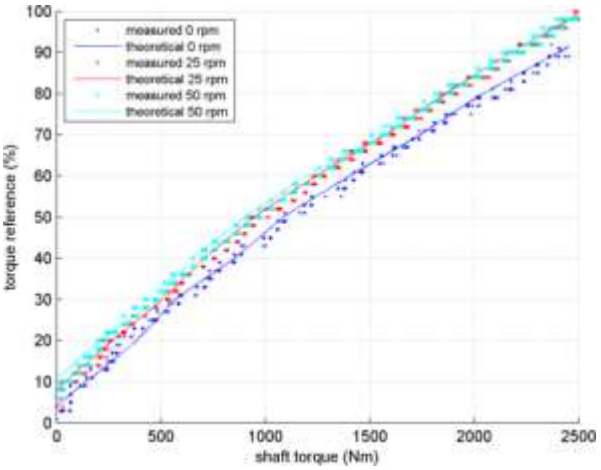

Figure 11 - VFD torque reference as function of shaft torque at zero, 25 and 50 RPM

IV - VALIDATION

After preparing the previously described approach, it was important to evaluate the ability of the developed rotor emulator (shaded blocks in Figure 12). This evaluation is performed by comparing theoretical torque values predicted by the rotor model with those measured by the torquemeter, during both steady and transient operating conditions produced by hardware-in-the-loop emulation.

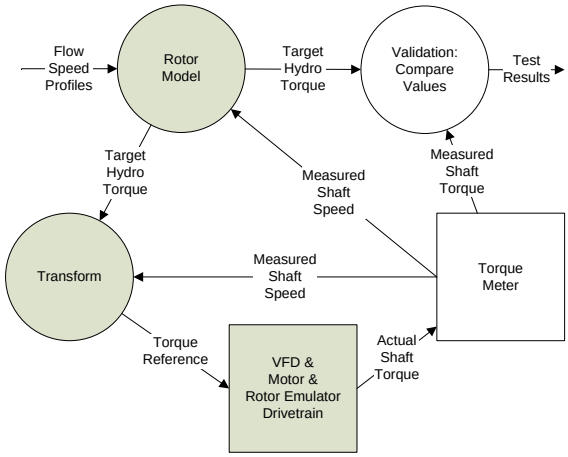

Figure 12 - Validation process block diagram

Three operational scenarios were selected to evaluate performance: locked rotor, spin-up/spin-down and power production in waves (Table 1). Each scenario represents a combination of turbine operation, flow conditions, and generator control. Rotor operation indicates anticipated operating states of an MHK turbine: either shaft braked, spinning up, spinning down, or normal operation. Flow conditions can vary as a velocity profile and/or wave conditions. The generator controller approach used for a scenario can vary as well, and is described in Table 1. Although rotor emulation performance was the primary purpose for evaluation, generator control algorithms are necessary for (and affect) the evaluation, and are therefore included.

Table 1 - Scenario criteria selected to evaluate rotor emulator performance.

	Rotor Operation	Flow	Generator Controller
Scenario 1	Braked rotor	Constant flow	Maintain zero speed
Scenario 2	Rotor spinning up/ down	Constant flow	Maximize gen. power production
Scenario 3	Rotor in oscillating flow	Simulated wind-driven waves	Maximize gen. power production

In Scenario 1, the generator is configured to maintain zero shaft speed using speed control. In Scenarios 2 and 3, the generator is configured with an industry-standard generator controller used by wind turbines [16]. This controller is designed to maximize generator power production under normal operating conditions. It maximizes power production by commanding electromechanical torque to maintain TSR for a maximal coefficient of power and is a non-adaptive, fixed-gain, region 2 controller.

Scenario 1: Locked Rotor

The locked-rotor scenario represents a situation where an OCT's rotor is not rotating and is held by generator and component friction, generator active control, or a mechanical brake. This scenario is important because hydrodynamic torque on stationary rotors is orders of magnitude smaller than a rotor's peak torque (see Figure 7) and therefore affects hydrodynamic response of a turbine. It is equally valuable to quantify this particular condition to determine a sufficient minimum torque to induce rotor rotation to establish cut-in speed criteria. Evaluating the locked rotor condition is also required to evaluate control techniques to hold a rotor stationary during extreme current events or during deployment and recovery states.

For this analysis, flow speed was incremented by 0.01 m/s for each execution cycle of 0.15 s, resulting in a flow acceleration of 0.067 m/s^2 (Figure 13). Mean theoretical torque was 216.2 Nm, while mean measured torque was 237.2 Nm. The difference between mean theoretical and

mean measured shaft torque was 20.9 Nm, yielding a percent error of 9.7%.

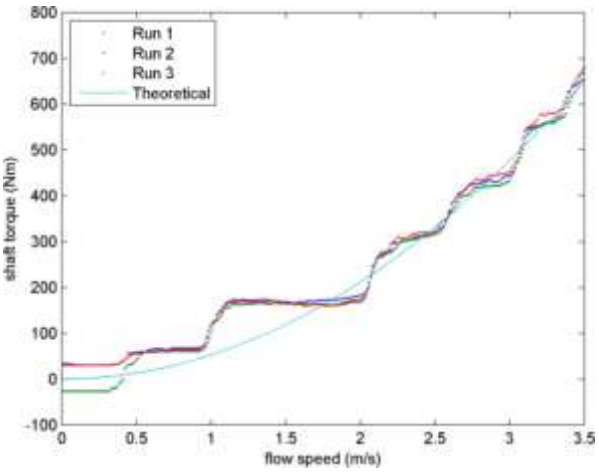

Figure 13 – Locked rotor condition imparted shaft torque in simulated ocean current vs. predicted shaft torque.

At simulated flow speeds of 0.5 m/s or less, the measured shaft torque does not match a low numerically-predicted hydrodynamic shaft torque (10 Nm for 0.5 m/s flow). Instead, constant non-zero shaft torques are examples of "locked-in torque" where torque remains "locked-in" among drivetrain components from previous rotations.

Results show that measured torque is greater than the theoretical hydrodynamic torque used to select torque references for flow speeds up to 1.7 m/s. These errors have a maximum value of 102.9 Nm, which occurred at a simulated flow speed of 1.2 m/s. This may indicate that the approach under-predicts flow speeds required to overcome static friction associated with turbine drivetrains. For flow speeds above 1.7 m/s, the model performs well in applying predicted locked rotor hydrodynamic shaft torque to the rotor shaft, with errors less than 44 Nm.

Scenario 2: Spin-Up/Spin-Down

Another important operating scenario which was evaluated is the transition between locked rotor operation and power production states. Figure 14 highlights a spin-up/spin-down scenario where the rotor emulator is started with a constant, simulated flow speed of 1.4 m/s. The spin-up portion of the run emulates releasing the OCT's brake in this flow. The rotor is allowed to spin-up, but is constrained by the region 2 generator controller described earlier. After near steady-state torque (approx. 1200 Nm) is achieved for 15 seconds, flow speed is decelerated to zero (at a rate of 0.067 m/s^2), allowing a spin-down state.

Mean theoretical torque for the run was 660 Nm, while mean measured torque was 624 Nm. The error between average theoretical and average measured torque was 36 Nm, yielding a percent error of 5.5%. The peak value calculated by the hydrodynamic model was 1298 Nm, and measured peak shaft torque produced by the rotor emulator was 1318 Nm. A maximum error of 438 Nm occurred 9.5 seconds into the run, nearly coincident with peak spin-up torque. The cross-correlation of these two signals showed that the greatest correlation occurred at a lag of 0.60 seconds. A maximum delay of 3.7 seconds occurred 1.6 seconds into the run. An average delay of 1.8 seconds during the first ten seconds confirms that the two signals are out-of-phase during spin-up.

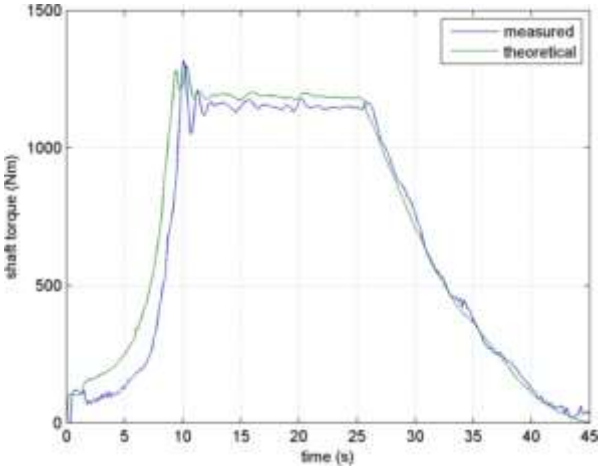

Figure 14 – Spin-up condition shaft torque (with region 2 controller in a 1.4 m/s flow), for theoretical hydrodynamic torque and measured shaft torque.

Scenario 3: Power Production in Perturbed Flow

The most common state expected for an OCT is in a steady current with possibly present wind-driven wave effects. To simulate this scenario, the generator is energized and commanded using the same fixed-gain controller utilized in scenario 2. Figure 15a presents a 60-second rotor emulator run with a 1.0 m/s current speed and a JONSWAP simulated wind-driven wave field (2 m significant wave height and a turbine hub depth of 10 m).

This scenario resulted in a mean theoretical hydrodynamic torque of 645 Nm, while the mean measured shaft torque was 612 Nm. The error between average theoretical and average measured torque was 34 Nm, yielding a percent error of 5.2%. A maximum error of 243 Nm occurred 56.8 seconds into the run. For comparison, the flow speed profile is plotted in Figure 15c. Cross-correlation between target and actual shaft torque (as function of lag) shows that greatest cross-correlation occurs at a lag of 0.75

seconds. This indicates that actual torque imparted by the rotor emulator is out of phase with the target by less than a second, and a satisfactory result.

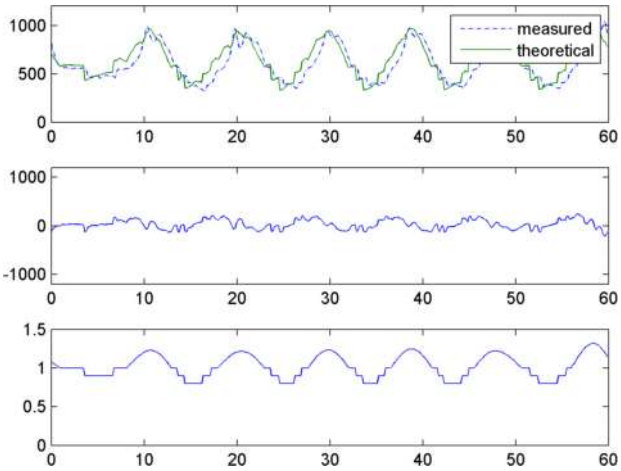

Figure 15 – Flow-perturbed operational scenario with simulated wind-driven waves; (a) top: theoretical and measured shaft torques; (b) middle: error between theoretical and measured shaft torque; (c) bottom: associated flow speed profile.

A summary of validation results for the three scenarios is presented in Table 2.

Table 2 - Validation Summary

	Max error (Nm)	Mean error (Nm)	Max. percent error	Lag (s)
Locked rotor	102.9	20.9	9.7%	N/A
Spin-up / spin-down	438.0	36.0	5.5%	0.6
Perturbed flow	243.1	33.7	5.2%	0.75

V - CONCLUSION

This study presented an approach for operating a dynamometer as a rotor emulator using commercial off-the-shelf components rather than relying on a custom solution. Software was developed to model in-stream flows and to model rotors with prescribed characteristics. Through experimental observation, relationships between torque reference and resulting physical shaft torque were identified over various ranges of operating speeds and torques. By applying curve-fitting and one-dimensional interpolation, a software transform was developed to determine VFD torque references needed to achieve actual shaft torques at dictated shaft speeds.

Rotor emulator performance was validated under various simulated conditions by measuring OCPGS ability to achieve target shaft torque on the physical system. Percent error between mean theoretical hydrodynamic torque and mean measured shaft torque data sets was 9.7% (locked rotor), 5.5% (spin-up/spin-down), and 5.2% (perturbed flow), indicating favorable results.

Future Work

Variable frequency drives offer simple motor control with speed or torque references as controller output. The present rotor-emulator transform uses only measured shaft speed in calculating a target torque reference. Future work will explore enhancing the rotor emulator controller by adding measured shaft torque feedback as well (Figure 16).

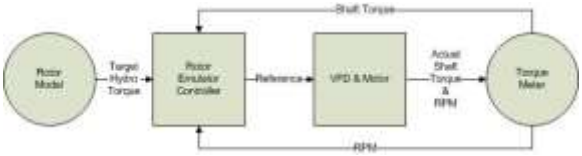

Figure 16 – Adding shaft torque feedback

Because filters can be effective in minimizing high-frequency excitation of a control system caused by feedback [17], future work will look at employing low-pass filters to condition the measured shaft speed feedback signal. Additional flow conditions (turbulence, non-axial, etc.) should be considered and added, as well, to more comprehensively emulate natural forcing.

The present study provides a first-look, high-level validation of the developed rotor emulator. To better validate transient behaviors (like those observed in Scenario 2), future work will be augmented with measures of traditional second-order system characteristics like rise time, time constant, and overshoot, etc.

And, finally, to improve the accuracy of generated torque reference values used by the rotor emulator, additional experimentation will be performed at minimum and maximum operating conditions to refine coefficients of the utilized polynomials.

Acknowledgements: The SNMREC is supported by the State of Florida and by the U.S. Department of Energy. The views expressed here are solely those of the authors.

REFERENCES

[1] J.H. VanZwieten Jr., W.E. Laing Jr., and C.R. Slezycki, "Efficiency Assessment of an Experimental Ocean Current Turbine Generator" in Proceedings of the IEEE Oceans Conference, Kona, Hawaii, September 19-22, no. 110422-215, 2011

[2] Waters, N., Beaujean, P.-P.J., Vendittis, D., "Detection, localization, and identification of bearing faults on an ocean turbine," Oceans, 2012 , vol., no., pp.1,8, 14-19 Oct. 2012 doi: 10.1109/OCEANS.2012.6404832

[3] Mjit, M., Beaujean, P.-P.J., Vendittis, D.J., "Smart Vibration Monitoring System for an Ocean Turbine," High-Assurance Systems Engineering (HASE), 2011 IEEE 13th International Symposium on , vol., no., pp.252,260, 10-12 Nov. 2011 doi: 10.1109/HASE.2011.34

[4] Cardei, I., Agarwal, A., Alhalabi, B., Tavtilov, T., Khoshgoftaar, T., Beaujean, P.-P., "Software and communications architecture for Prognosis and Health Monitoring of ocean-based power generator," Systems Conference (SysCon), 2011 IEEE International , vol., no., pp.353,360, 4-7 April 2011 doi: 10.1109/SYSCON.2011.5929092

[5] Caraiman, G., Nichita, C., Minzu, V., Dakyo, B., Jo, C. H., "Real time marine current turbine emulator: Design, development and control strategies," *Electrical Machines (ICEM), 2012 XXth International Conference on* , vol., no., pp.2145,2150, 2-5 Sept. 2012 doi: 10.1109/ICElMach.2012.6350179

[6] Neammanee, B., Sirisumrannukul, S., Chatratan, S., "Development of a Wind Turbine Simulator for Wind Generator Testing", International Energy Journal 8 (2007) 21-28.

[7] J. Neely, K. Ruehl, R. Jepsen, J. Roberts, S. Glover, M. Horry, F. White; "Electromechanical Emulation of Hydrokinetic Generator for Renewable Energy Research", Proceedings of the IEEE OCEANS Conference, September 2013, San Diego, CA

[8] M. Borghi, F. Kolawole, S. Gangadharan, A. Engblom, J. VanZwieten, G. Alsenas, W. Baxley, and S. Ravenna (2012) "Design, fabrication and installation of a hydrodynamic rotor for a small-scale experimental ocean current turbine" Proceedings of the IEEE SoutheastCon, Orlando, Florida, March 15-18, no. SECon.2012.6196973

[9] "Labview system design software, national instruments." http://www.ni.

[10] "Matlab the language of technical computing, the mathworks,inc., 3 apple hill drive, natick, ma 01760-2098usa." info@mathworks.com

[11] Ocean Engineering Science, Bernard Le Mehaute, Daniel M. Hanes, Harvard University Press, Jan 1, 1990, pp 303-305

[12] R. G. Dean and R. A. Dalrymple, Water wave mechanics for engineers and scientists. River Edge, NJ: World Scientific, 1991, pp. 86

[13] Buhl, M. L., 2004, "WT_Perf User's Guide," NWTC Design Codes, Available: http://wind.nrel.gov/designcodes/simulators /wtperf/. Last modified Dec-2004; accessed 11-February-2011.

[14] J.H VanZwieten, C.M. Oster, A.E.S. Duerr, (2011) "Design and analysis of a rotor Blade optimized for extracting energy from the Florida Current", Accepted to the 30th International Conference on Ocean, Offshore, and Arctic Engineering, June 19-24, Rotterdam, The Netherlands, no. OMAE2011-49140

[15] Sale, D. C., 2010, "HARP_Opt User's Guide," NWTC Design Codes, Available: http://wind.nrel.gov/designcodes/simulators /HARP_Opt/ . Last modified 27-July-2010; accessed 17-August-2010.

[16] Johnson, K. E. (2004), "Adaptive Torque Control of Variable Speed Wind Turbines", 107 pp.; NREL Report No. TP-500-36265, National Renewable Energy Laboratory, Golden, CO 80401

[17] Jonkman, J., Butterfield, S., Musial, W., and Scott, G. (2009), "Definition of a 5-MW Reference Wind Turbine for Offshore System Development", NREL Technical Report No. NREL/TP-500-38060, February 2009, National Renewable Energy Laboratory, Golden, CO 80401

View publication stats